A Novel Oscillator Design with Metamaterial-Möbius Coupling To a Dielectric Resonator

Ulrich L. Rohde, Ajay K. Poddar

Abstract

With the aid of a Metamaterial-Möbius coupling mechanism, these fundamental-frequency dielectric-resonator oscillators operate through X-Band with low phase noise and superior figure of merit (FOM). Manipulating and tailoring the electromagnetic wave coupling properties, several interesting properties of Metamaterial-Möbius Strips (MMS) envisage, such as reduction in the size for a given operating frequency and suppression of spurious resonance modes, thereby improving the figure of merit (FOM) of tunable oscillator. FOM can be a limiting factor in modern communications systems, especially those that rely on power efficient low phase noise signal source. Phase noise can increase the bit error rate (BER) of a telecommunications link, degrade the stability of beams in particle accelerators, and degrade the sensitivity of radar systems. Phase noise is an oscillator parameter that grows in importance with the complexity of modern communications modulation formats. Fortunately, work on Metamaterial-Möbius coupling inspired dielectric resonator oscillators (DROs) by us has resulted in a line of compact surface-mount DROs with extremely low phase-noise levels at fundamental-frequency outputs through 8 GHz and higher, suitable for use in commercial, industrial, and military applications.

Introduction

These new DROs, based on the DRO in the previous chapter rely on planar resonators based on metamaterial Möbius strips (MMS), which are simple examples of anholonomy. Therefore it was possible to maintain the phase noise in a much smaller package compared to the previous example.

The geometrical phenomenon of anholonomy depends on the failure of a quantity to recover its original value, when the parameters on which it depends are varied around a closed circuit [1]-[3].

Metamaterials are engineered periodic composites that have negative refractive-index characteristics not available in natural materials [4]-[7]. Such composite materials, in typical topological arrangements can achieve values of negative permeability (-μ) and negative permittivity (-ε) [8]. In general, the refractive index of a medium can be characterized by four possible sign combinations for the permeability-permittivity pair ($\mu\epsilon$), and can be described [9]-[18] by means of Eqs. 1-4

$$n = \sqrt{(+\epsilon)(+\mu)} = +\sqrt{\mu\epsilon} \rightarrow \text{(DPS: double +ve material)} \quad (1)$$

$$n = \sqrt{(-\epsilon)(+\mu)} = j\sqrt{\mu\epsilon} \rightarrow \text{(ENG: epsilon -ve material)} \quad (2)$$

$$n = \sqrt{(-\epsilon)(-\mu)} = -\sqrt{\mu\epsilon} \rightarrow \text{(DNG: double -ve material)} \quad (3)$$

$$n = \sqrt{(+\epsilon)(-\mu)} = j\sqrt{\mu\epsilon} \rightarrow \text{(MNG: mu -ve material)} \quad (4)$$

where ε_o is $8.85\text{x}10^{-12}$ and $\mu_0 = 4\pi\text{x}10^{-7}$, n is refractive index of the medium.

Equation 1 is valid for double positive substrate (DPS) materials, with permittivity and permeability both positive; Eq. 2 is valid for epsilon negative (ENG) substrate materials, with negative permittivity and positive permeability; Eq. 3 is for double negative (DNG) substrate materials, with permittivity and permeability both having negative values; and Eq. 4 is for mu negative (MNG) substrate materials, where the permeability is negative but the permittivity has positive values.

The DNG materials described by Eq. 3 are typically defined as artificial materials and commonly referred to as "metamaterials" in the technical literature. In addition, they are called left-handed materials (LHMs), negative index materials (NIMs), and backward-wave materials (BWMs) [19]. The unusual characteristics of metamaterials, such as backward-wave propagation, exhibit group velocity characteristics in a direction opposite to that of its phase velocity, causing strong localization and enhancement of fields. This can result in significant enhancement of a resonator's quality factor (Q), if losses can be minimized [20].

The realization of true DNG material (metamaterial) is questionable. In general, it is difficult to build a material or medium simultaneous with negative permittivity and negative permeability for broad operating frequency ranges from a set of arbitrary passive structure unit cells arranged in pre-determined order. This may lead to a violation of energy conservation principle at the intersecting plane between a right-handed material (RHM) and LHM media because of the generation of energy.

An attempt to build the DNG material or medium—based on the fact that for a specific orientation and arrangement of the passive structure, the values of permittivity and permeability diminish as the frequency increases—has been applied to demonstrate virtual negative permittivity and permeability at specific frequencies, but it lacks validity for broadband operation. In reality, it is easier to demonstrate independently negative permeability or negative permittivity, but achieving both negative characteristics in a DNG material can be difficult.

Printed multi-coupled slow-wave resonators exhibit improved Q-factor characteristics, and are commonly employed in low-phase-noise oscillator applications.21 For example, improvement in the Q-factor of a slow-wave resonator (λ/4 coplanar stripline) can be realized by forming an open- circuit load where the incident and reflected electromagnetic (EM) waves move entirely in-phase with each other. In reality, such open-circuit conditions are difficult to maintain over a desired frequency band.

In addition, the implementation of a λ/4 coplanar strip-line circuit on a substrate can increase the overall size of the circuit. Insertion of additional floating metal shields may help alleviate some of the problems with slow-wave circuit designs [21]-[25].But negative - permeability - based planar split - ring-resonator (SRR) structures and complementary split-ring-resonator (CSRR) structures can enable compact on-chip implementations of these circuits, with promising and cost-effective solutions for metamaterial oscillator and filter applications [26]-[29].

In the proper arrangement, planar SRR and CSRR structures can achieve independently negative permeability and negative permittivity at the resonance needed to create optimum coupling for a disc resonator in a high-performance DRO. These structures can be characterized as magnetic and electric dipoles excited by the magnetic (H) and electric (E) fields along the ring axis [7].

Interestingly, a single-negative property (ε or μ) supported by an SRR (split-ring resonator) or CSRR (complementary split-ring resonator) structure can yield a sharp stopband in the vicinity of the resonant frequency, enabling storage of EM energy into an SRR or CSRR structure through an evanescent-mode coupling mechanism, resulting in high Q. It should be noted that the Q multiplier effect does not violate the law of conservation of energy since the evanescent mode in SRR stores energy but does not transport energy [21].

Figure 1 shows a typical differential transmission-line-loaded, SRR-based metamaterial resonator oscillator. For a differential (push-pull) oscillator, the incident wave energy injected by the cross-coupled inverters propagates in forward waves along the transmission line towards the circuit's short point; the energy is reflected at the SRR load, and the reverse wave has a superposition of the incident wave and leads to a resonance when in phase. Stronger wave reflection means less loss and higher resonator Q [20].

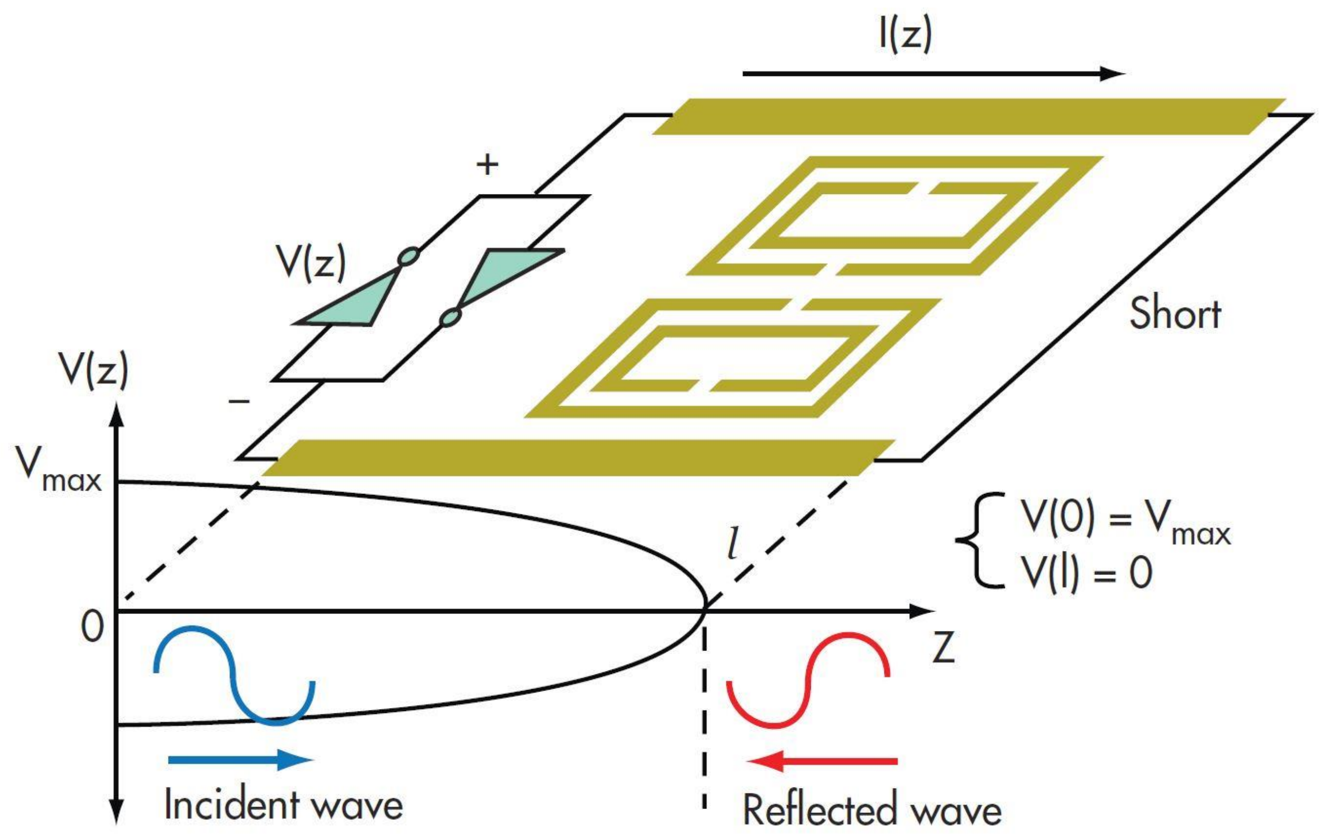

Figure 1 A typical simplified representation of differential transmission line based SR [20]

When working with artificial composite materials, the negative permeability response can be manipulated by including electrically small resonant shapes, such as split rings. Figure 2 depicts a typical SRR structure for the realization of tunable μ ($\mu < 0$) and ε ($\varepsilon < 0$) characteristics for applications in tunable oscillator circuits [17]-[18].

Möbius strips offer unique characteristics, including self-phase-injection properties along the mutually coupled surface of the strips, enabling enhanced Q for a given size of printed transmission-line resonator. The oscillator's loaded Q_L is described by Eqs. 5 and 6:

$$Q_L = \frac{\omega_0}{2}\left|\frac{d\varphi(\omega)}{d\omega}\right|_{\omega=\omega_0} = \frac{\omega_0}{2}\tau_d; \quad \tau_d = \left|\frac{d\varphi(\omega)}{d\omega}\right|_{\omega=\omega_0} \tag{5}$$

$$\tau_d = \frac{d\varphi(\omega)}{d\omega}\bigg|_{\omega=\omega_0} = \frac{\varphi(\omega_0+\Delta\omega)-\varphi(\omega_0-\Delta\omega)}{2\Delta\omega} \tag{6}$$

where $\varphi(\omega)$ is the phase of the oscillator's open loop transfer function at a steady state and τ_d is the group delay of the metamaterial Möbius strips resonator.

Figure 3 shows a typical metamaterial-based, Möbius-strip resonator and its equivalent lumped-element model circuits. From Eqs. 5 and 6, by introducing mode injection into metamaterial Möbius strips, phase-dispersion, loss, and group delay can be optimized.

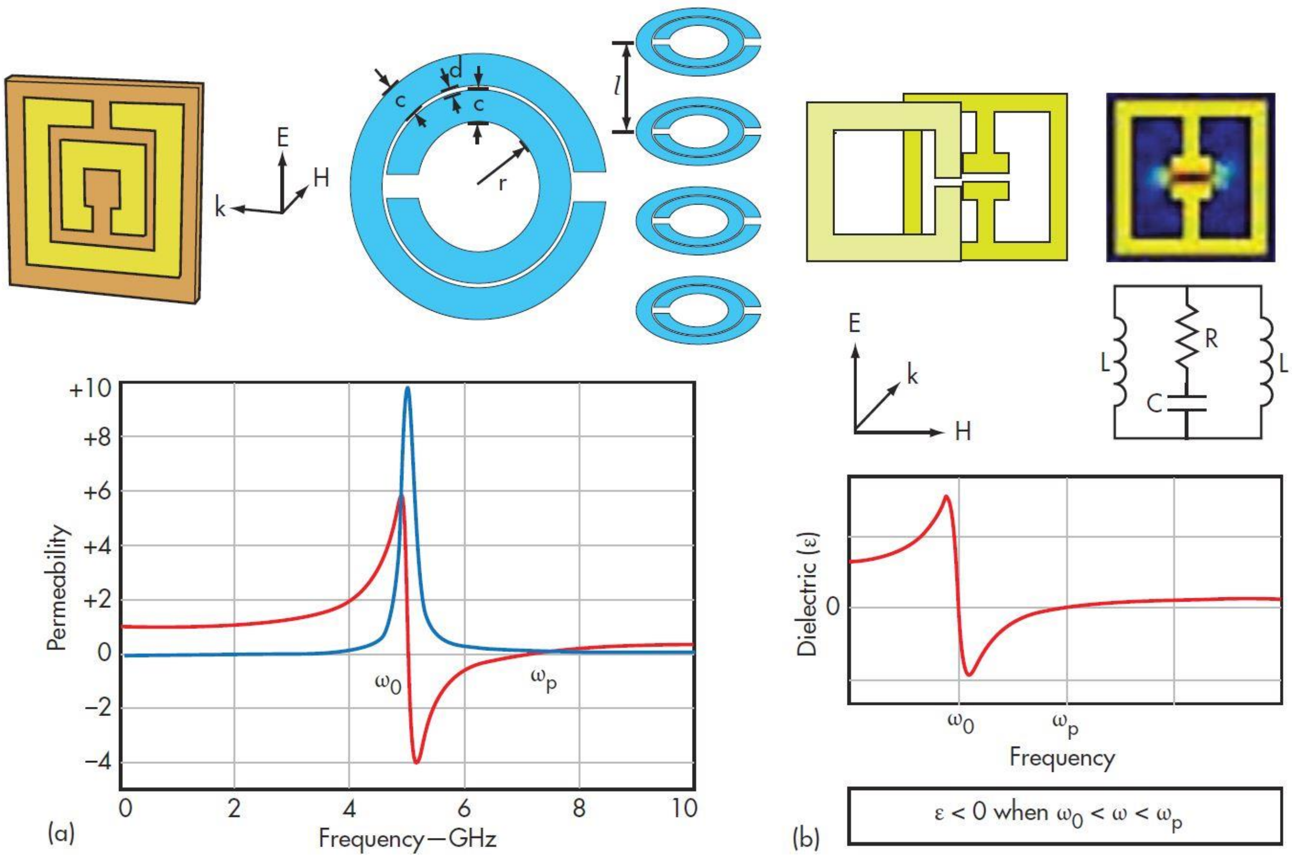

Fig. 2 A typical SRR structure exhibits the tunable characteristics for permeability (a) for μ (μ < 0) near resonance condition and (b) for permittivity ε (ε < 0) near resonance condition [17]-[18].

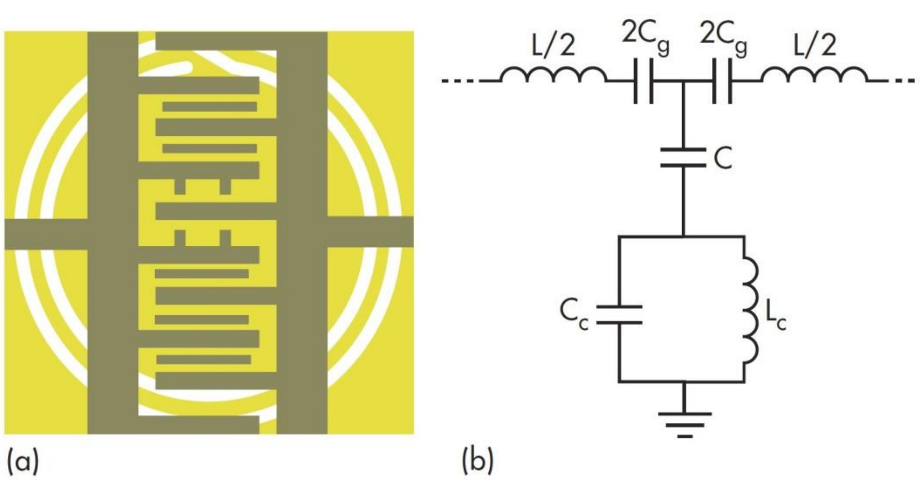

Figure 3: These diagrams show a typical Metamaterial based Möbius strips resonator: (a) layout and (b) electrical equivalent lumped-element model circuits.

Figure (4) shows the typical arrangement of varactor-tuned metamaterial resonator utilizing SRR. Utilizing Varactor diodes can improve the tuning range but maintaining the effective negative index properties of the resonator network is a challenging task. As shown in Figure (4), coupled SRR is being realized for improving the effective negative index characteristics without degrading the quality factor. Figure (5) shows the coupled SRRs for the realization of Möbius coupling for enhancing evanescent mode energy based on energy harvesting techniques (transformation of unwanted modes and dissipated energy into MMR (Metamaterial-Mobius Resonator) cavity.

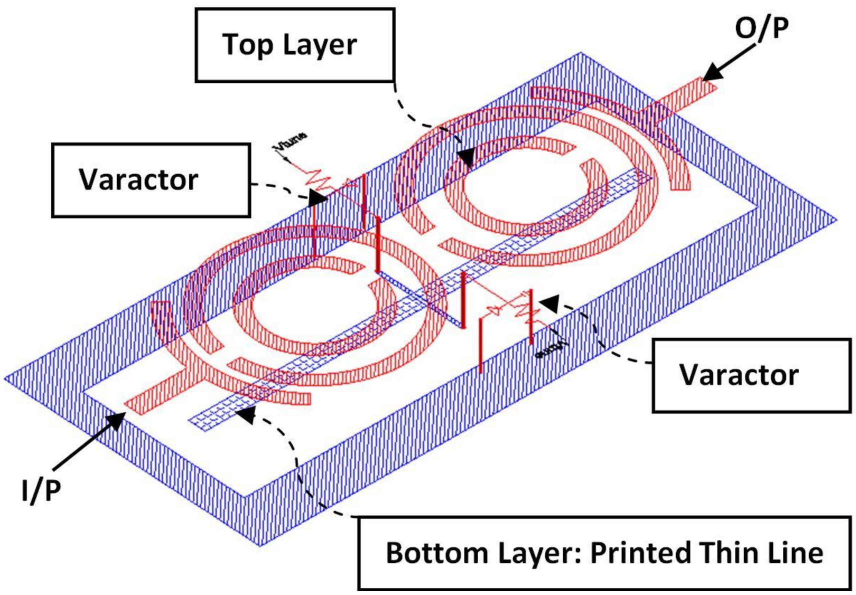

Fig.4: A typical Varactor-tuned metamaterial resonator comprised of coupled split-rings resonator (SSR) network.

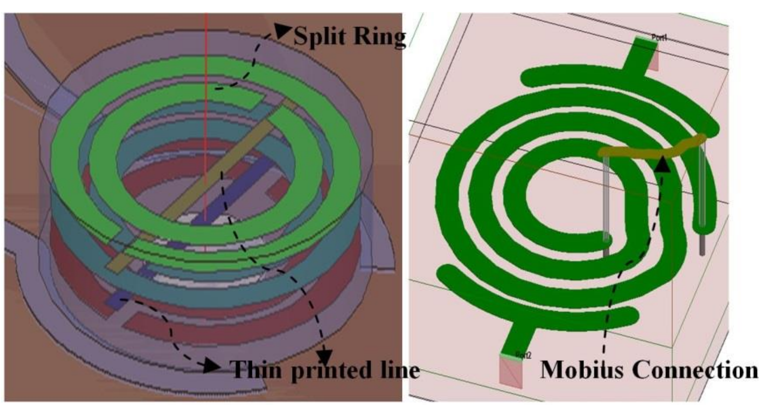

Fig.5: shows a typical printed coupled line structure : (a) Transverse coupled metamaterial resonator using SRR and thin printed line, and (b) Möbius Strips

Figure (6) shows the typical DRO for the understanding of the DR (dielectric resonator) placement on the PCB (printed circuit board). It can be noticed that typically DR (dielectric resonator) is in disk configuration, attached through spacer made of low dielectric material. As shown in Figure (6), with the help of screw mounted on DR, frequency can be tuned for narrow band applications. However, DR placement using spacer/puck for optimum coupling and mechanical screw for tuning is sensitive to frequency drift under vibration. For applications where g-sensitivity is a critical issue; DRO inherently exhibits poor phase noise performance in presence of vibration and acceleration. Figure (7) shows the typical schematic of DRO using disc in conjunction with stacked SRR for the realization of Metamaterial-Möbius inspired SRR for frequency shaping resonant module, yielding stable oscillator circuits for applications as LO (local oscillators) [21].

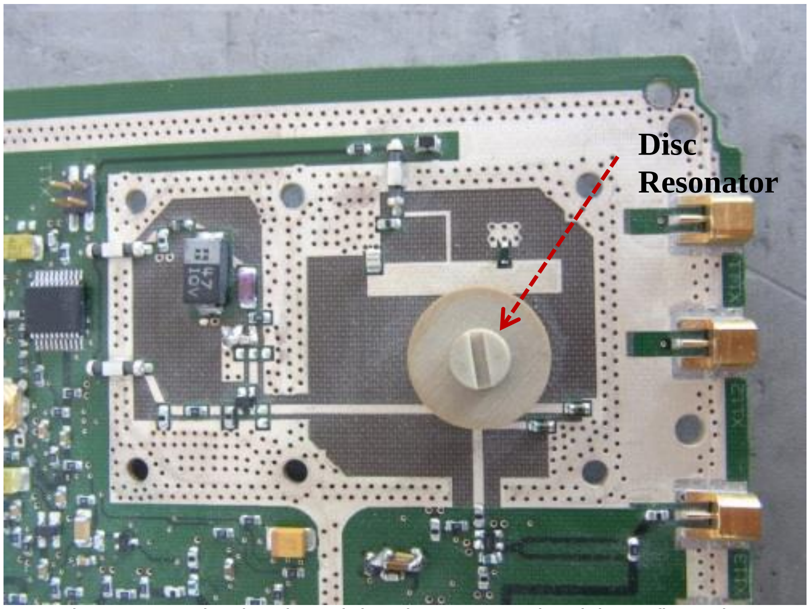

Fig. 6: DRO circuit using Dielectric resonator in Disk configuration

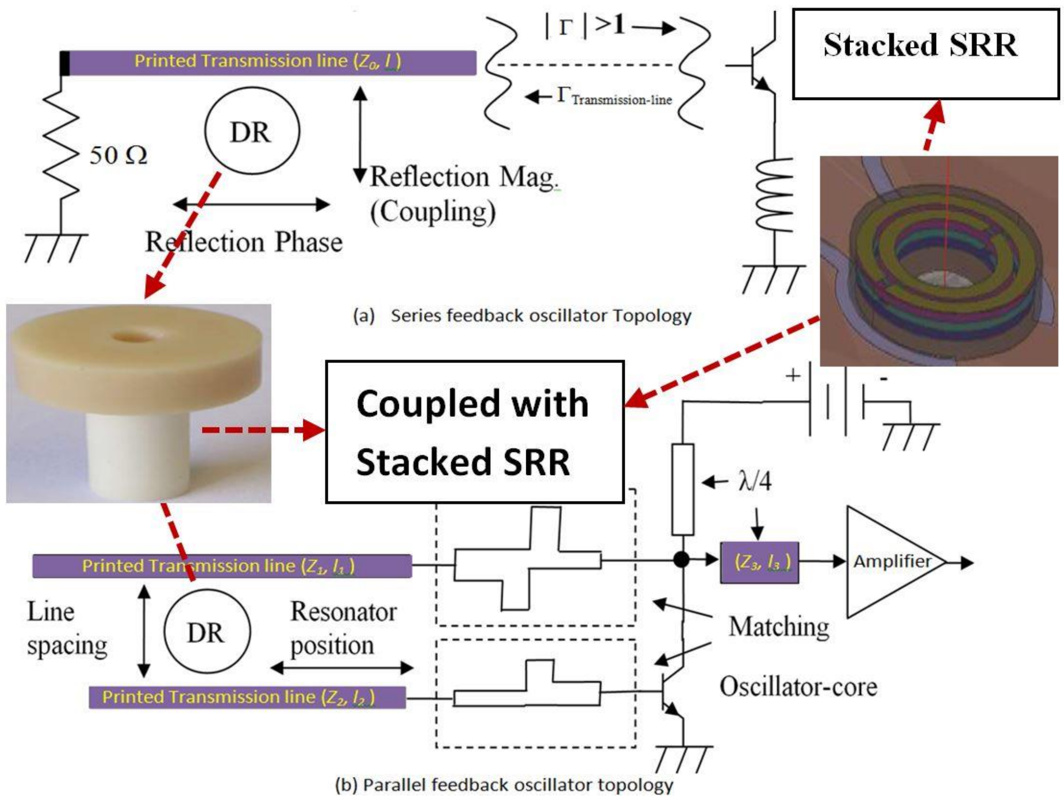

Fig.7: A typical DRO circuit: (a) Series feedback (Reflection type), and (b) parallel feedback (Transmission type)

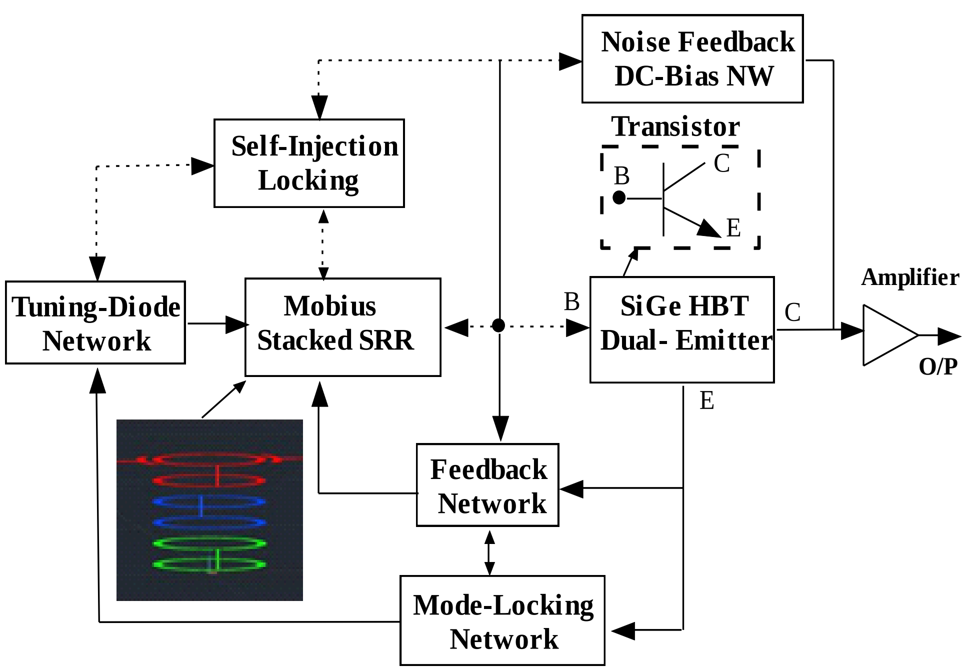

Fig. 8: shows the block diagram of the Mobius stacked SRR K-band oscillator

For applications requiring compact size DROs, Metamaterial-Mobius DROs have been developed in SMD housings measuring just 0.75×0.75 in square packages. These oscillators can be extended to any number of fixed frequencies, typically from 3 to 18 GHz, without long lead times required to produce the sources. Figure 9 depicts the specification and phase noise plot for model SDR0800-8, operating at 8 GHz in SMD housings measuring just 0.75×0.75 in square packages.

SPECIFICATIONS

Frequency	8 GHz
Tuning Voltage	1 - 10 VDC
Bias Voltage	+8 VDC @ 25 mA (Max.)
Output Power	+1 dBm (Min.)
Tuning Sensitivity	1.5 MHz/V (Typ.)
Thermal Drift	2 ppm / °C (Typ.)
Output Impedance	50 Ohms (Nom.)
Harmonic Suppression	34 dBc (Typ.)
Frequency Pulling	500 kHz (Typ. @ 1.75:1 VSWR)
Frequency Pushing	400 kHz/V (Typ.)
Tuning Port Capacitance	10 pF (Typ.)
Modulation Bandwidth	> 20 MHz

Phase Noise

Offset	dBc/Hz (Typ.)
10 kHz	-114
100 kHz	-140
1 MHz	-160
10 MHz	-170

Phase Noise

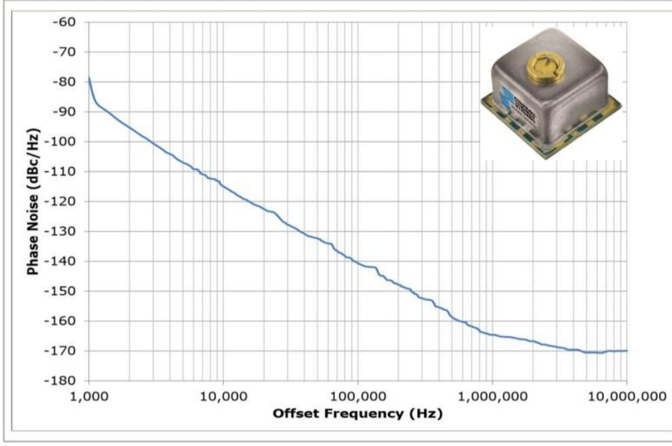

Figure 9 depicts the specification and phase noise plot for model SDR0800-8

These oscillators should be powered by a clean DC bias voltage; otherwise an external regulator should be employed to minimize variations in supply voltage. A DRO factory set for an output frequency of 10 GHz, for example, can be mechanically adjusted by about ±50 MHz.

An electrical tuning port provides an adjustment range of ±1 MHz with tuning voltages of +1 to +15 VDC to compensate for frequency drift in phase-locked systems. The supply-current is typically 30 mA and the temperature range is specified from -25 to +70°C.

References

1. U.L. Rohde and A. K. Poddar, “DROs drop phase noise”, Microwave & RF, pp. 80—84, Feb 2013.
2. A. K. Poddar, U.L. Rohde, and D. Sundarrajan, “A Novel Mobius-Coupled Printed Resonator Based Signal Sources,” 2013 IEEE MTT-S Digest, June 2013, pp. 1-3.
3. U. L. Rohde and A. K. Poddar, “A Novel Evanescent-Mode Mobius-Coupled Resonator Oscillators,” IEEE Joint UFFC Symposia with European Frequency and Time Forum (EFTF) and Piezo response Force Microscopy, July 21-25, 2013.
4. V. Veselago, “The electrodynamics of substances with simultaneously negative values of ‘ε’ and μ,” Soviet Physics-Solid State, Vol. 8, No. 12, 1967, pp. 2854–2856.
5. V. G. Veselago, “The electrodynamics of substance with simultaneously negative values of ε and μ”, Soviet Physics Uspeki, Vol. 10, 1968, pp. 509–514.
6. J. B. Pendry, A. J. Holden, D. J. Robbins, and W. J. Stewart, “Magnetism from conductors and enhanced nonlinear phenomena,” IEEE Transactions on Microwave Theory & Techniques, Vol. 47, 1999, pp. 2075–2084.
7. R. A. Shelby, D. R. Smith, and S. Schultz, “Experimental verification of a negative index of refraction,” Science Vol. 292, 2001, pp. 77–79.
8. J. Manuel and T. Alves, “Metamaterials with Negative Permeability and Permittivity: Analysis and Application,” M. S. thesis, University Tecnica de Lisboa Instituto Superior Tecnico, 2010.

9. U. L. Rohde, A. K. Poddar, T. Itoh, and A. Daryoush, “Evanescent-Mode Metamaterial Resonator Based Signal Sources,” IEEE IMaRC Delhi, December 14-16, 2013.
10. U. L. Rohde, A. K. Poddar, T. Itoh, and A. Daryoush, “Evanescent-Mode Metamaterial Resonator Based Signal Sources,” IEEE IMaRC Delhi, December 14-16, 2013.
11. A. K. Poddar, U. L. Rohde, and T. Itoh, “Metamaterial Mobius Strips (MMS): Tunable Oscillator Circuits,” Proceedings of the 2014 International Microwave Symposium, Tampa, FL, June 2014.
12. C.-T. M. Wu, A. K. Poddar, U. L. Rohde, and T. Itoh, “A C-band Tunable Oscillator Based on Complementary Coupled Resonator using Substrate Integrated Waveguide Cavity,” submitted to European Microwave Symposium 2014.
13. M. Martin et al., “Miniaturized coplanar waveguide stop band filters based on multiple tuned split ring resonators,” IEEE Microwave & Wireless Component Letters, Vol. 13, 2003, pp. 511–513.
14. Joan et al., “Microwave filters with improved stopband based on sub wavelength resonators,” IEEE Transactions on Microwave Theory & Techniques, Vol. 53, 2005, pp. 1997–2006.
15. Bonache et al., “Novel microstrip bandpass filters based on complementary split-ring resonators. IEEE Transactions on Microwave Theory & Techniques, Vol. 54, 2005, pp. 265–271.
16. J. B. Pendry, A. J. Holden, D. J. Robbins, and W. J. Stewart, “Magnetism from conductors and enhanced nonlinear phenomena,” IEEE Transactions on Microwave Theory & Techniques, Vol. 47, 1999, pp. 2075–2084.
17. J. B. Pendry, “Negative Refraction Makes a Perfect Lens,” Physical Review Letters, Vol. 85, No. 18, October 2000.
18. J. B. Pendry, A. J. Holden, D. J. Robbins, and W. J. Stewart, “Low frequency plasmons in thin-wire structures,” Journal of Physics: Condensed Matter, Vol. 10, No. 22, June 1998, pp. 4785–4809.
19. W. Fei Shang et al., “96-GHz oscillators by high Q-Differential Transmission Line Loaded with Complementary Split-Ring Resonator in 65-nm CMOS,” IEEE Transactions on Circuits and Systems-II, Express Briefs, Vol. 60, No. 3, March 2013, pp. 127-131.
20. Y. Shang et al., “Design of High-Q Millimeter-Wave Oscillator by Differential Transmission Line Loaded with Metamaterial Resonator in 65-nm CMOS,” IEEE Transactions on Microwave Theory & Techniques, Vol. 61, No. 5, May 2013, pp. 1892-1902.
21. A. K. Poddar, “Slow Wave Resonator Based Tunable Multi-Band Multi-Mode Injection-Locked Oscillators,” Dr.-Inh.-habil thesis, BTU Cottbus, Germany (draft thesis submitted for defense on Jan 2013).